

A rad-hard, 60 μm pixel sensor optimized for the direct detection of electrons

M. Sannino^a, A. Bofill-Petit^a, M. Giulioni^a, A. Mollà Garcia^a, and R. Turchetta^{a*}, G. McMullan^b and R. Henderson^b, C. Copetti^c, B. Janssen^c, L. Mele^c and G. van Duinen^c

a: IMASENIC, Pl. Tetuan 40-41, 08010 Barcelona, Spain

b: Laboratory of Molecular Biology, Cambridge, UK

c: ThermoFisher Scientific, Eindhoven, NL

* Tel: +34 935466100

Email: renato.turchetta@imasenic.com

Abstract — Today CMOS Image Sensors (CIS) are the solution of choice for the direct detection of electrons for Transmission Electron Microscopes (TEM). Existing CIS products are optimized for relatively high energy electrons, normally around 300 keV. In this paper we describe the design and performance of a prototype designed for lower energy, around 100 keV. The prototype was designed with a pitch of 60 μm and manufactured with substrates with different thicknesses of the epitaxial layer. The prototype sensor of 70x70 pixels was manufactured in a 180 nm CIS process. The measured detective quantum efficiency at zero spatial frequency DQE(0) is $98\pm 3\%$. The sensor was irradiated with $9.6\cdot 10^9$ electrons per pixel: at this dose some minor degradation occurred which was fully recovered after two days of annealing at room temperature.

I. INTRODUCTION

Today CIS are the solution of choice for the direct detection of electrons for Transmission Electron Microscopes (TEM)¹. Existing direct detection CIS products are optimized for relatively high energy electrons, normally around 300 keV. At these energies, the trajectories of electrons are relatively little affected by the silicon layer, so that the combination of thinned detector (of the order of a few tens of μm)² and smallish pixels (in between 5 and 15 μm in size) are used. High-energy cryo-TEMs with CIS imaging have produced a breakthrough in the field of structural biology^{3, 4}, allowing a growing number of complex molecular structures to be reconstructed, and among the latest achievements, the first ever detection of the molecular structure of the COVID19 spike protein and

the COVID19 RNA polymerase can be quoted⁵. These kinds of results make Cryo-TEM's highly desirable for structural biology. Because of their popularity, there is a strong market pull for a more affordable cryo-TEM to also serve the laboratories without access to the funding required for a high-energy cryo-TEM. Recently⁶, it was shown that lower energy electrons, around 100 keV, can also provide the image quality that is required for some of the biological research. This finding paves the way to the development of dedicated 100 keV entry-level cryo-TEMs to respond to the strong market pull for a more affordable cryo-TEM to also serve the laboratories without access to the funding required for a high-energy cryo-TEM.

II. SIMULATION

When moving from 300 down to 100 keV, the energy loss of electrons in matter undergo a rapid change: the amount of energy released per unit path is much higher as well as the scattering⁷. The rapid increase in the energy loss can be seen in Figure 1 below, showing results from our simulation. The average energy lost by electrons while penetrating in silicon increases almost linearly up to a maximum depth, after which it drops very rapidly to zero as a result of the electrons having been stopped in the material. The increased scattering means that as the electrons traverse the silicon, the position where the charge is created can be far apart from where the electrons enter the silicon. The optimal pixel size will then depend on the thickness of the epitaxial layer.

In order to optimize the sensor, we developed a simulation where individual electrons are followed in

¹ A. R. Faruqi, R. Henderson, G. McMullan, *Progress and Development of Direct Detectors for Electron Cryomicroscopy*, Advances in Imaging and Electron Physics, Volume 190, 2015

² D. Contarato et al., *High Speed, Radiation Hard CMOS Pixel Sensors for Transmission Electron Microscopy*, Physics Procedia 37 (2012) 1504 – 1510

³ W. Kühlbrandt, *The Resolution Revolution*, Science, 28 Mar 2014, Vol. 343, Issue 6178, pp. 1443-1444

⁴ N. Guerrini, R. Turchetta, G. Van Hofen, A. R. Faruqi, G. McMullan, R. Henderson, *A 61mmx63mm, 16Million Pixels, 40*

Frames per Second, Radiation-Hard CMOS Image Sensor for Transmission Electron Microscopy, R47 Proceedings of International Image Sensor Workshop, Hokkaido, Japan

⁵ <https://www.thermofisher.com/blog/microscopy/>

⁶ M. Peet, R. Henderson, C. J. Russo, *The energy dependence of contrast and damage in electron cryomicroscopy of biological molecules*, Ultramicroscopy, Vol. 203, August 2019, Pages 125-131

⁷ D. Durini (editor), *High Performance Silicon Imaging: Fundamentals and Applications of CMOS and CCD sensors*, Chap. 10, Woodhead Publisher, 2014

their path through silicon. At every step, they lose energy, thus generating electron-hole pairs. Using a semi-analytical model for the drift diffusion of the charge carriers, the amount of charge seen by each pixel is determined. The electronics performance of the sensor is added to give a simulated image of electrons' hits, from which quantities like detection efficiency and spatial resolution can be determined.

Figure 2 shows an example of the simulated energy loss. On the right, there is a peak corresponding to electrons which have been fully absorbed. In this case, the electrons generate $100,000/3.6=27,777$ electron-hole pairs. Electrons which are not fully absorbed generate a distribution skewed towards higher energy losses with respect to the most probable energy loss. This curve is similar to the well-known Landau distribution⁸, which describes the energy loss of charged particles traversing a material.

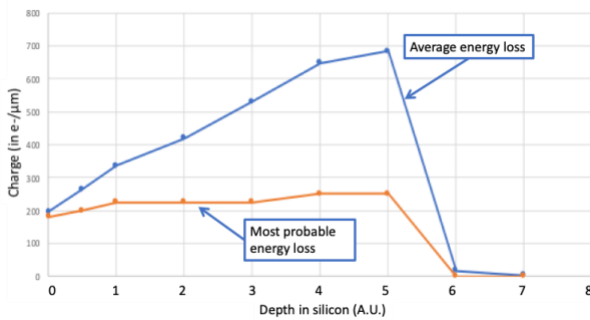


Figure 1. Simulated energy loss of 100keV electrons as a function of their depth in silicon.

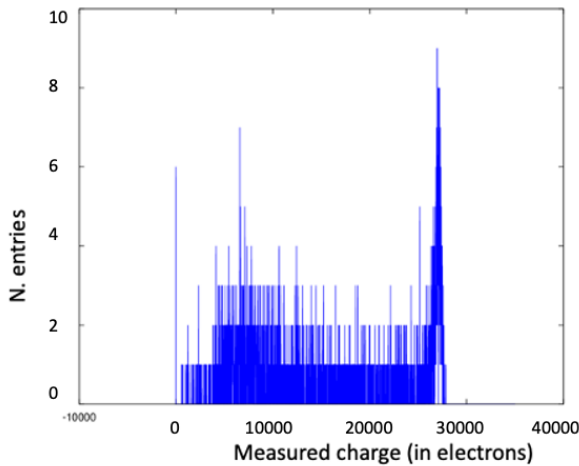


Figure 2. Simulated distribution of the amount of measured charge. The peak at the right corresponds to electrons being fully stopped in the epi layer.

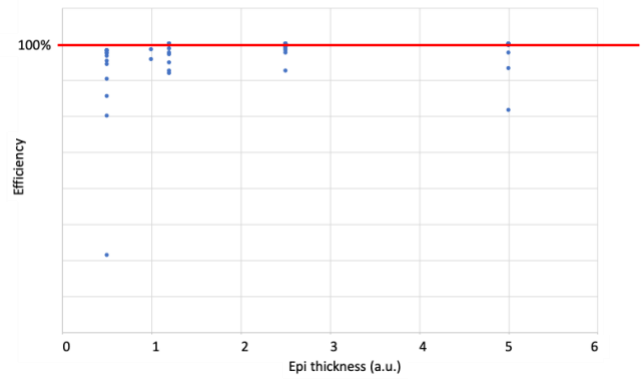


Figure 3. Detection efficiency as a function of epi thickness. Each dot corresponds to a different simulated sensor configuration.

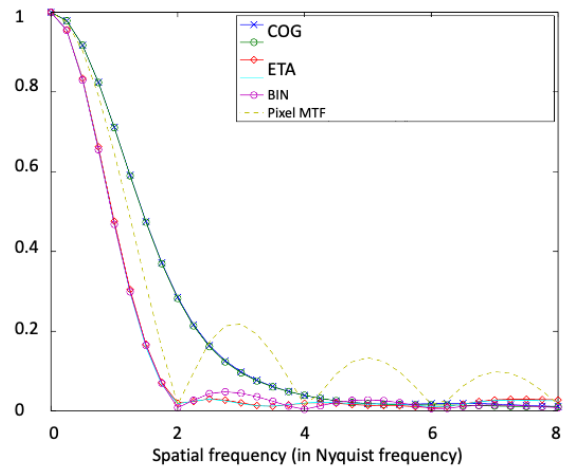


Figure 4. Simulated MTF for different position finding algorithms.

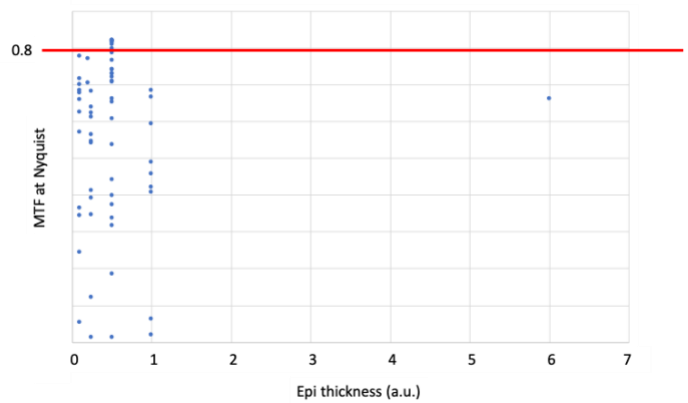


Figure 5. MTF at Nyquist vs epi thickness. The way the position of impact of single electrons is calculated affects the MTF.

Many different sensor configurations were generated, varying parameters like the sensor pitch, the epitaxial thickness and resistivity, the thickness of the entrance window and the diode bias. A summary of the detection efficiency at 0 spatial frequency DQE(0) is

⁸ H. Bichsel, *Straggling in thin silicon detectors*, Rev. Mod. Phys., Vol. 60, No. 3, July 1988

shown in Figure 3. The figure shows that if the detector is thick enough, it is possible to achieve 100% efficiency.

For many sensor configurations, the charge generated by one electron spreads over several pixel. It is then possible to use different algorithms for the calculation of the impact point. The simplest (*Binary*) algorithm is to assign the impact point to the center of the pixel with the highest signal. In the Center-of-gravity (*COG*) algorithm, the position is simply calculated by using all the pixels with a non-zero signal and weighing their position according to the amount of charge. A non-linear algorithm (*ETA*) that takes into account the non-linear effect of charge drift-diffusion can also be applied. By summing up the response of many simulated electrons, a modulation transfer function MTF can be determined. An example of the variation of the MTF for a given sensor and for different position finding algorithm is shown in Figure 4. Figure 5 shows how the MTF at Nyquist varies for different sensor configurations and as a function of the thickness of the epitaxial layer. A high value, in excess of 80%, can be obtained.

III. THE PROTOTYPE

A prototype sensor was designed and manufactured in a 180nm CIS technology. The floorplan of the sensor is shown in Figure 6. The sensor is readout through a single analogue port and achieve 500 fps. It was manufactured with three different epi thicknesses. In Figure 8, the measured gain and equivalent noise charge is shown for different prototypes with the three combinations of epi thicknesses and resistivity. Using the photon transfer curve method, the electro-optical parameters of sensor were measured using visible and infra-red light.

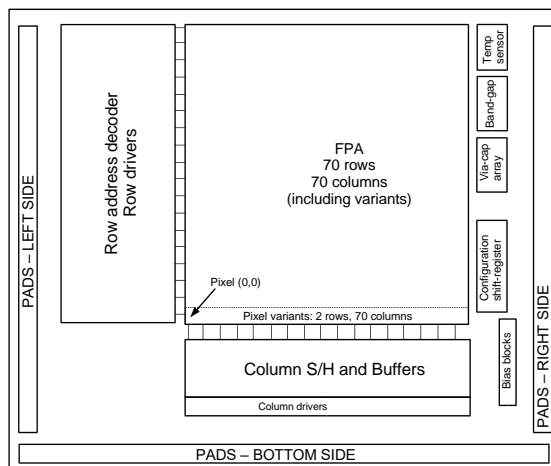


Figure 6. Floorplan of the prototype sensor.

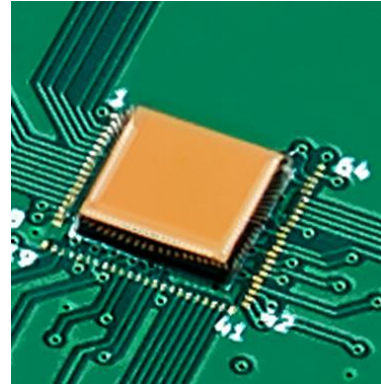


Figure 7. Photo of the low energy TEM prototype

The gain varies between 8.5 and 9 $\mu\text{V}/\text{e}$, giving a total voltage signal for fully absorbed electrons between 236 and 250 mV. The equivalent noise charge is around 60 e- rms, corresponding to a signal-over-noise ratio for a single 100 keV electron of 462, assuming that the entire energy is deposited in one pixel. The linear full well capacity (Figure 9) is around 40 and 50 thousand electrons depending on the different pixel configuration, corresponding to 1.4 and 1.8 of the charge released by a single fully absorbed electron.

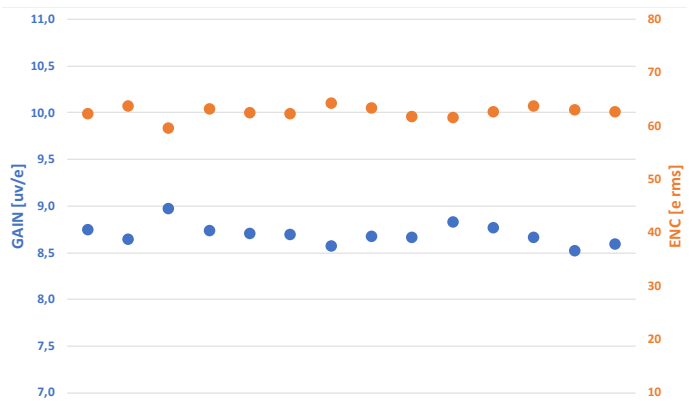


Figure 8. Gain and ENC measured for different sensors. Each point along the horizontal axis correspond to a different sensor.

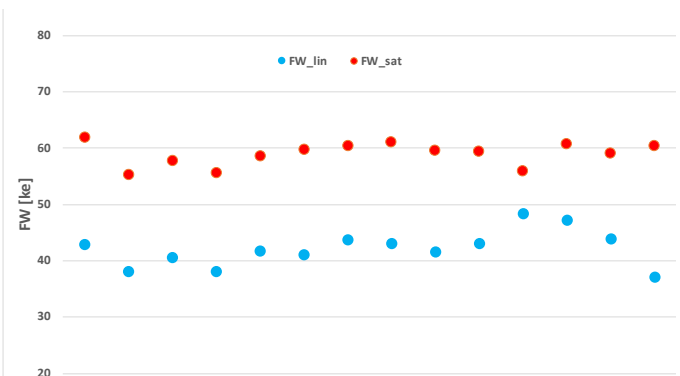


Figure 9. Full well linear and at saturation, as measured in different sensors. The linearity of the sensor was measured to be 1% and the FPN was 0.02%. Each point along the horizontal axis correspond to a different sensor.

The sensor was tested in an electron microscope model Philips CM200-FEG. Examples of recorded frames are shown in Figure 11 for the three different epitaxial layer thicknesses. They show the number of pixels with a non-zero charge varies depending on the substrate type.

The measured energy loss is shown in Figure 10. The curves show similar features as the simulated one. On the right is a peak corresponding to full absorption and on the left is the distribution corresponding to electrons which were not fully absorbed. The dotted lines show the corresponding distribution when the energy of the beam is reduced from 100 to 60 keV.

The measured MTF is shown in Figure 12 both in integrating and counting mode. In integrating mode, the image is composed by summing the charge of the electrons from several frames, while in counting mode, individual electrons are counted and their position is summed up to make the final image.

The sensor was irradiated with $9.6 \cdot 10^9$ electrons per pixel in a few minutes. Some leakage current increase occurred but it was fully recovered after annealing during two days at room temperature. Measured energy loss distribution before and after irradiation are shown for one substrate and one energy in Figure 13.

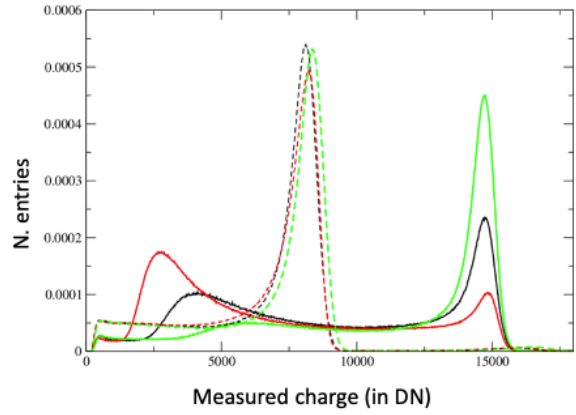


Figure 10. Measured charge in a TEM. Solid lines are for 100keV and dotted lines for 60 keV measurements. Red is the thinnest and green is the thickest epi.

IV. CONCLUSIONS

On the basis of these results, a wafer-scale, high speed sensor, optimized for low energy cryo-TEM is going to be developed. In order to achieve high speed for a stitched sensor, a modified stitching⁹ will be adopted so that the long readout lines can be split in the middle and the sensor can be read at both ends.

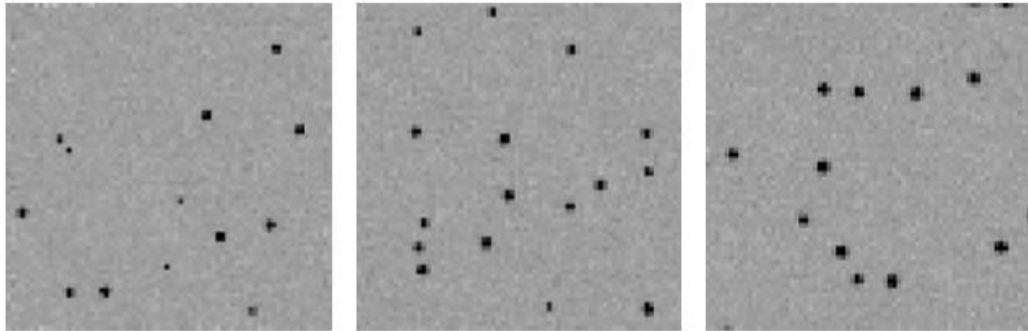


Figure 11. Images of single electrons, detected in epi layers with different thicknesses: the thinnest is on the left and the thickest is on the right.

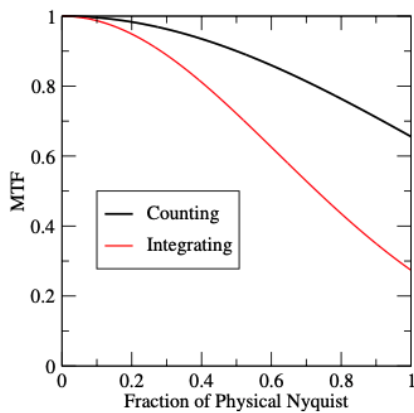


Figure 12. MTF measured in a TEM.

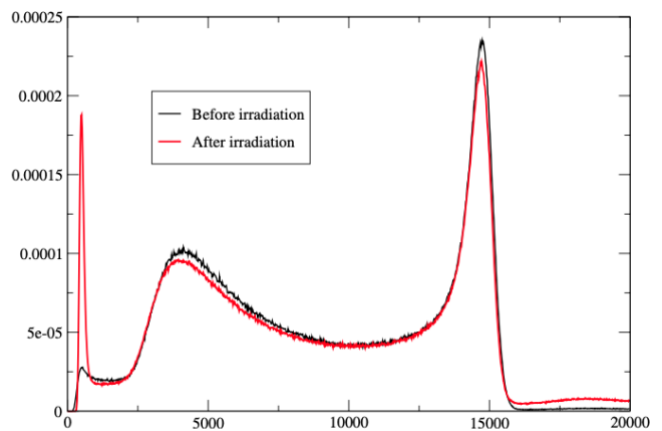


Figure 13. Measured charge before and after irradiation.

⁹ R. Turchetta, EP20382222, 24/3/2020